AIP | Journal of Applied Physics

Broadband negative permeability using hybridized metamaterials: Characterization, multiple hybridization, and terahertz response

Nguyen Thanh Tung, Bui Son Tung, Ewald Janssens, Peter Lievens, and Vu Dinh Lam

Citation: Journal of Applied Physics **116**, 083104 (2014); doi: 10.1063/1.4893719
View online: http://dx.doi.org/10.1063/1.4893719
View Table of Contents: http://scitation.aip.org/content/aip/journal/jap/116/8?ver=pdfcov
Published by the AIP Publishing

Articles you may be interested in

Metamaterial composite bandpass filter with an ultra-broadband rejection bandwidth of up to 240 terahertz
Appl. Phys. Lett. **104**, 191103 (2014); 10.1063/1.4875795

Meta-atom cluster acoustic metamaterial with broadband negative effective mass density
J. Appl. Phys. **115**, 054905 (2014); 10.1063/1.4864135

Fabrication of large-area 3D optical fishnet metamaterial by laser interference lithography
Appl. Phys. Lett. **103**, 123116 (2013); 10.1063/1.4821508

An ultrathin and broadband metamaterial absorber using multi-layer structures
J. Appl. Phys. **114**, 064109 (2013); 10.1063/1.4818318

Enhancement of evanescent waves in waveguides using metamaterials of negative permittivity and permeability
Appl. Phys. Lett. **84**, 669 (2004); 10.1063/1.1645658

AIP | Journal of Applied Physics

Journal of Applied Physics is pleased to announce André Anders as its new Editor-in-Chief

[This article is copyrighted as indicated in the article. Reuse of AIP content is subject to the terms at: http://scitation.aip.org/termsconditions. Downloaded to] IP: 84.194.89.79 On: Mon, 25 Aug 2014 18:07:57

Broadband negative permeability using hybridized metamaterials: Characterization, multiple hybridization, and terahertz response

Nguyen Thanh Tung,[1,2,a)] Bui Son Tung,[1] Ewald Janssens,[2] Peter Lievens,[2] and Vu Dinh Lam[1,b)]
[1]*Institute of Materials Science, Vietnam Academy of Science and Technology, Vietnam*
[2]*Laboratory of Solid-State Physics and Magnetism, KU Leuven, B-3001 Leuven, Belgium*

(Received 1 July 2014; accepted 11 August 2014; published online 25 August 2014)

There is an increased interest to create artificial magnetic metamaterials that show a negative permeability over a wide frequency range. In this paper, we experimentally and numerically demonstrate a broadband negative permeability using symmetric cut-wire-pair metamaterial structures. This finding is based on the second-order hybridization, which is activated by manipulating the correlation between the coupling within a single cut-wire pair and the coupling between neighboring cut-wire pairs. An effective medium analysis is performed to identify the role of the internal and external interactions in the hybridized metamaterials. An extended second-order hybridization scheme is proposed, which describes the electromagnetic response of more complex systems that exhibit an extremely wide band of negative permeability. In addition, the terahertz response of the cut-wire-pair dimer is further explored by scaling down the dimensions of the structures. © *2014 AIP Publishing LLC*. [http://dx.doi.org/10.1063/1.4893719]

I. INTRODUCTION

Creating unusual macroscopic effective properties by structural design is an important advance in metamaterials (MMs). Since the first observation of the fascinating negative refractive-index property, the so-called left-handed behavior, MMs have been in the spotlight.[1,2] In general, a negative index of refraction is achieved if the material simultaneously has a negative permeability, produced by an artificial magnetic resonance, and a negative permittivity, yielded by a metallic plasma behavior.[1] While broadband negative permittivity is commonly obtained by employing the low-frequency plasma of a continuous-wire medium,[3] the bandwidth of negative permeability structures is often narrow due to the resonant nature.[4] Obviously, negative refractive MMs with a broad operating band are more useful for applications and therefore broadband magnetic MMs have been a topic of particular interest.[5–10]

So far, the most common way to create broadband magnetic resonances is by integrating individual resonant structures in one unit cell. However, this approach often results in multiple and separated resonances rather than a true broadband behavior.[6–10] Having these separated resonances closer requires rigorous geometric adjustments as well as symmetry breaking, which is a serious challenge for current fabrication techniques. In some cases, the extension of unit cell dimensions and the asymmetry of transmission due to structural inhomogeneity might break the validation of the effective medium principle.[11]

In the search for alternatives to the current approaches, we recently have introduced a general mechanism to achieve broadband negative permeability using a cut-wire-pair (CWP) dimer.[12] By exploiting the interaction between two identical CWP monomers, a hybridized magnetic resonance is predicted to split up and the frequency range that shows a negative permeability becomes wider.

In this work, we report a comprehensive study to elaborate the above mentioned idea. The samples are fabricated and their transmission spectra are measured at microwave frequencies and compared with numerical simulation data. The calculated effective negative permeability demonstrates broadband behavior. An effective medium analysis is performed to manifest the central role of coupling interactions in hybridized CWP trimers, which extends the hybridization picture for more complex CWP arrangements. Finally, we rescale the dimensions of CWP systems to examine the validity of the proposed hybridization scheme in the terahertz regime.

II. EXPERIMENTAL AND SIMULATION SETUP

Figure 1(a) illustrates a unit cell of the CWP dimer and the electromagnetic polarization. The CWP dimer consists of two identical CWP monomers, which are composed of a dielectric spacer sandwiched between two copper rectangles. The periodicities of the unit cell in the x and the y directions are $a_x = 3.5$ mm and $a_y = 7.0$ mm, respectively. The dielectric layer is made of FR4 with a dielectric constant of 4. The length l and the width w of the copper cut-wires are 5.5 and 1.0 mm, respectively. With these parameters the CWP exhibits a known magnetic resonance at 13.8 GHz.[13,14] The thickness of the dielectric medium between the two wires of a CWP and the distance between the two layers of the CWP dimer are denoted as t_d and d, respectively. The simulations were carried out based on the finite integration technique (CST Microwave Studio). Periodic boundary conditions are applied in the x and y directions.

A one-sided photo of an actual sample and the experimental setup are shown in Fig. 1(b). The transmission

[a)]tungnt@ims.vast.ac.vn
[b)]lamvd@ims.vast.ac.vn

 © 2014 AIP Publishing LLC

[This article is copyrighted as indicated in the article. Reuse of AIP content is subject to the terms at: http://scitation.aip.org/termsconditions. Downloaded to] IP: 84.194.89.79 On: Mon, 25 Aug 2014 18:07:57

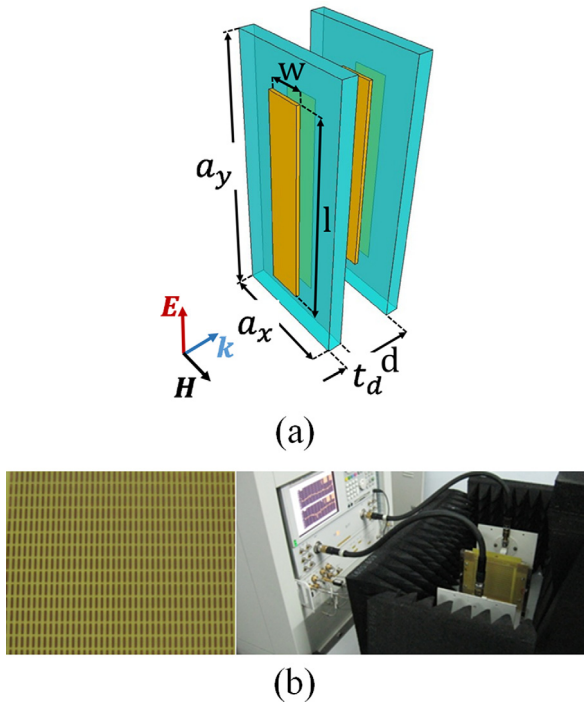

FIG. 1. (a) Unit cell of the CWP dimer sample and polarization of the electromagnetic radiation. (b) MMs sample composed of CWP structures (left) and experimental setup for the transmission measurements (right).

measurements are performed using a Hewlett-Packard E8362B network analyzer connected to microwave standard-gain horn antennas, which yield an electromagnetic wave in a frequency range of 12–18 GHz. The MMs samples are kept balance by a sample holder placed between the two antennas. The sample holder is made of glass, which is perfectly transparent in the frequency range of interest. The entire measurement setup is shielded by absorption plates to reduce the influence of background noise.

III. RESULTS AND DISCUSSIONS

The response of complex structures can be described by the electromagnetic analogue of molecular orbital theory.[15] In this model, the total energy of the complex structure is considered as a hybridization of characteristic energies corresponding to each constituent elemental structure. Under normal incidence of electromagnetic plane waves, a plasmonic response is induced in each individual cut-wire (CW). The electromagnetic response of the CWP monomer is a hybridization of two individual plasmon modes.[16–18] According to the hybridization scheme, there are two stimulated eigenmodes with opposite current directions. The antisymmetric mode, induced by an attractive force corresponding to the out-of-phase charge oscillations, has a lower energy ($|w_-\rangle$) than the symmetric ($|w_+\rangle$) mode which corresponds to in-phase charge oscillations. While the symmetric mode operates as two electric dipoles, the antisymmetric mode with antiparallel currents behaves as an effective magnetic resonance. The energetic splitting of two modes is larger if the distance between the CWs (t_d) is smaller.[17]

The hybridization picture can also be applied to create higher order eigenmodes in a CWP dimer.[12] The electromagnetic response of the CWP dimer can be predicted using a second-order hybridization scheme as shown in Fig. 2. Two factors contribute to the electromagnetic interactions in the CWP dimer: the internal coupling between two CWs in a pair and the external coupling between two CWPs in a dimer. When the external coupling is absent, the CWP dimer exhibits an original magnetic resonance ($|w_-\rangle$). If the external coupling between two CWPs is increased, the originally degenerate magnetic resonance will split into two second-order eigenmodes ($|w_{--}\rangle$ and $|w_{-+}\rangle$). For the CWP dimer, the thickness of the dielectric spacer t_d determines the internal coupling, while the distance between the CWP layers d determines the external coupling. Depending on the strength of the second-order hybridization, the magnetic resonance is slightly split or two entirely separated modes are present. Our previous simulation study predicted that the magnetic resonance of a CWP dimer starts splitting if d is of the same order of magnitude as t_d.[12] Hence, manipulating the ratio of d/t_d must be the key to reveal the picture of the second-order hybridization.

Two series of experiments and simulations are carried out to demonstrate the influence of the internal/external coupling ratio on the magnetic resonance of the CWP dimer: (i) tuning the distance between CWPs in the dimer (d) and (ii) tuning the distance between CWs in monomers (t_d). Figures 3(a) and 3(b) present the simulated and experimental transmission spectra according to d/t_d with t_d fixed at 0.4 mm. It is shown that when the external coupling strength is considerably weaker than the internal one ($d/t_d = 5$), the CWP dimer exhibits the original magnetic resonance peak at 13.8 GHz. If the external coupling is strengthened by decreasing d/t_d, the resonance gradually broadens. When the external and internal coupling strength are comparable ($d/t_d = 1$), the resonant splitting is almost complete (minima are appearing at 13.4 and 14.2 GHz) and a broadband

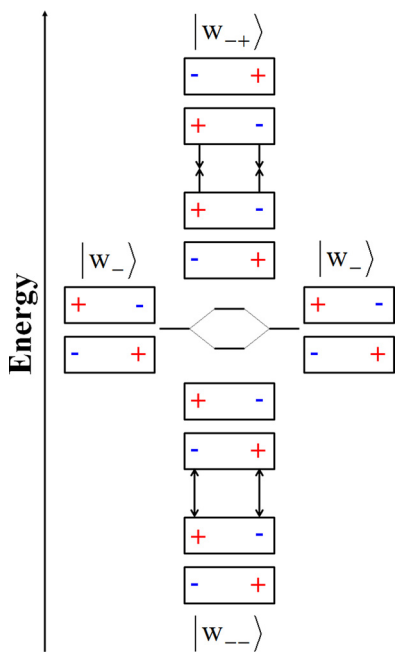

FIG. 2. Hybridization scheme of a CWP dimer.

[This article is copyrighted as indicated in the article. Reuse of AIP content is subject to the terms at: http://scitation.aip.org/termsconditions. Downloaded to] IP: 84.194.89.79 On: Mon, 25 Aug 2014 18:07:57

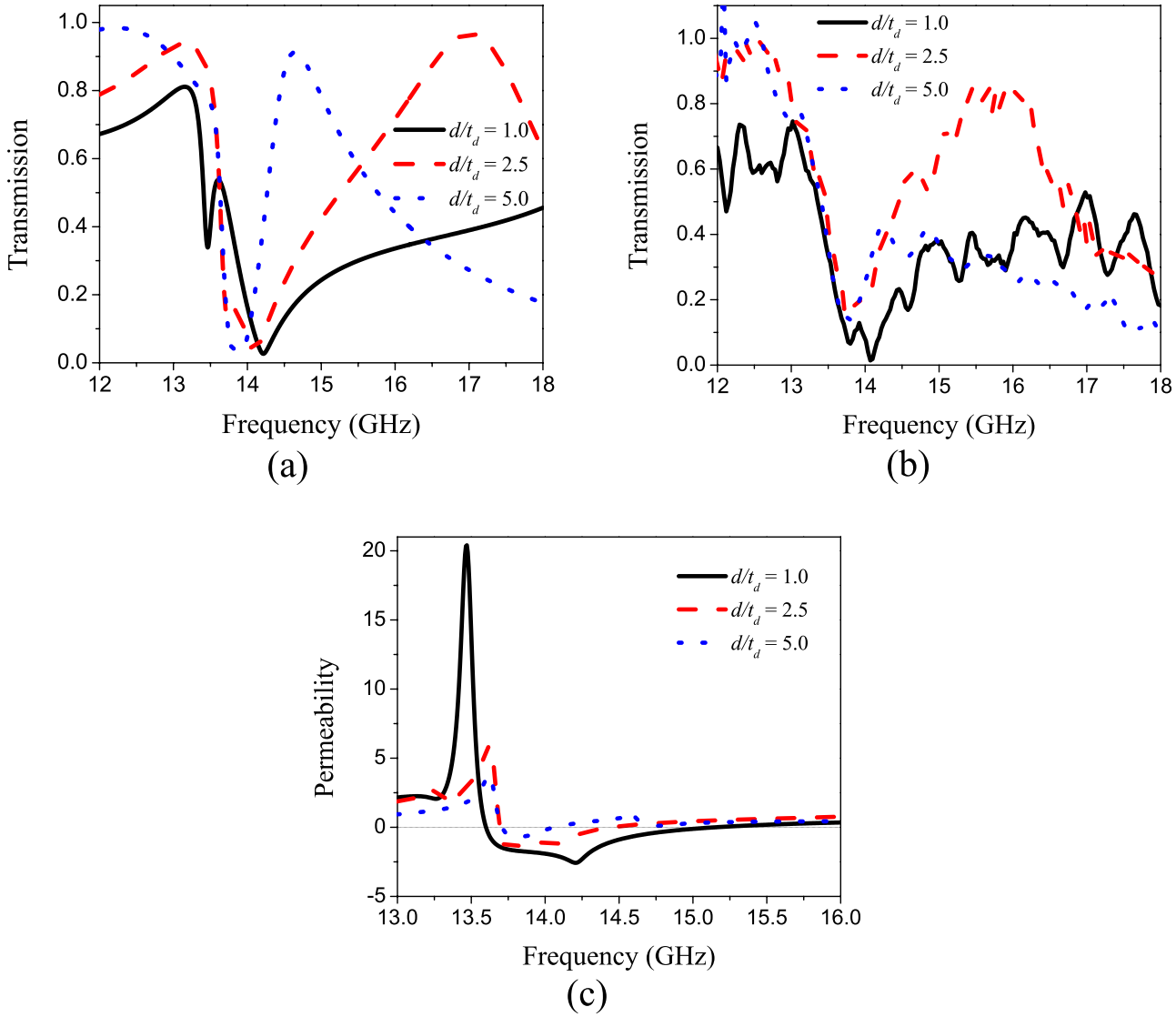

FIG. 3. (a) Simulated and (b) experimental transmission according to d/t_d. (c) Dependence of calculated permeability on d/t_d. t_d is kept at 0.4 mm while d is varied. All other parameters are unchanged.

resonance is achieved. The resonant splitting is not completely resolved in the experimental measurements. However, the broadening effect is clearly observed in both the experimental and simulated results. In order to confirm the origin of the resonance broadening, we calculate the permeability [see Fig. 3(c)] based on the simulated transmission data using the standard retrieval procedure.[19] Clearly, the magnetic resonance starts splitting with decreasing d/t_d and the negative permeability band is considerably broader when d is comparable to t_d.

In the second series of experiments and simulations, the influence of the internal/external coupling ratio on the resonance band is investigated by changing t_d while fixing $d = 1.6$ mm. Figures 4(a) and 4(b) show the simulated and measured transmission spectra of the CWP dimer as function of d/t_d. Obviously, the resonant band is significantly wider when d/t_d goes from 8 to 1.6. The experimental data are partially reiterated from the results reported in Ref. 20. The splitting of the resonance starts occurring in the simulated spectra at around $d/t_d = 2.0$ (with transmission minima at 13.6 and 14.4 GHz), in agreement with theoretical predictions.[12] With the hybridization picture in mind, one can imagine that increasing t_d results in a weaker strength of the internal coupling between two CWs in a monomer. Once the internal coupling strength is comparable to the external one, the second-order hybridization is activated that splits off the original magnetic resonance of the CWP structure and makes the resonant band broader. Although the resonant split is not obvious in the experimental spectra, it is verified by the calculated permeability in Fig. 4(c). By increasing t_d the negative permeability band splits and is extended because the second-order hybridization is stronger.

The results in Figs. 3 and 4 manifest that the electromagnetic response of the CWP dimer can be expressed via the interplay between the internal and external couplings. The broadband negative permeability is activated only when these two interactions are energetically comparable to each other. In both series, the bandwidth of the negative permeability region increases significantly (from about 3% to 13%) when decreasing the ratio d/t_d from 8 to 1. In good

[This article is copyrighted as indicated in the article. Reuse of AIP content is subject to the terms at: http://scitation.aip.org/termsconditions. Downloaded to] IP: 84.194.89.79 On: Mon, 25 Aug 2014 18:07:57

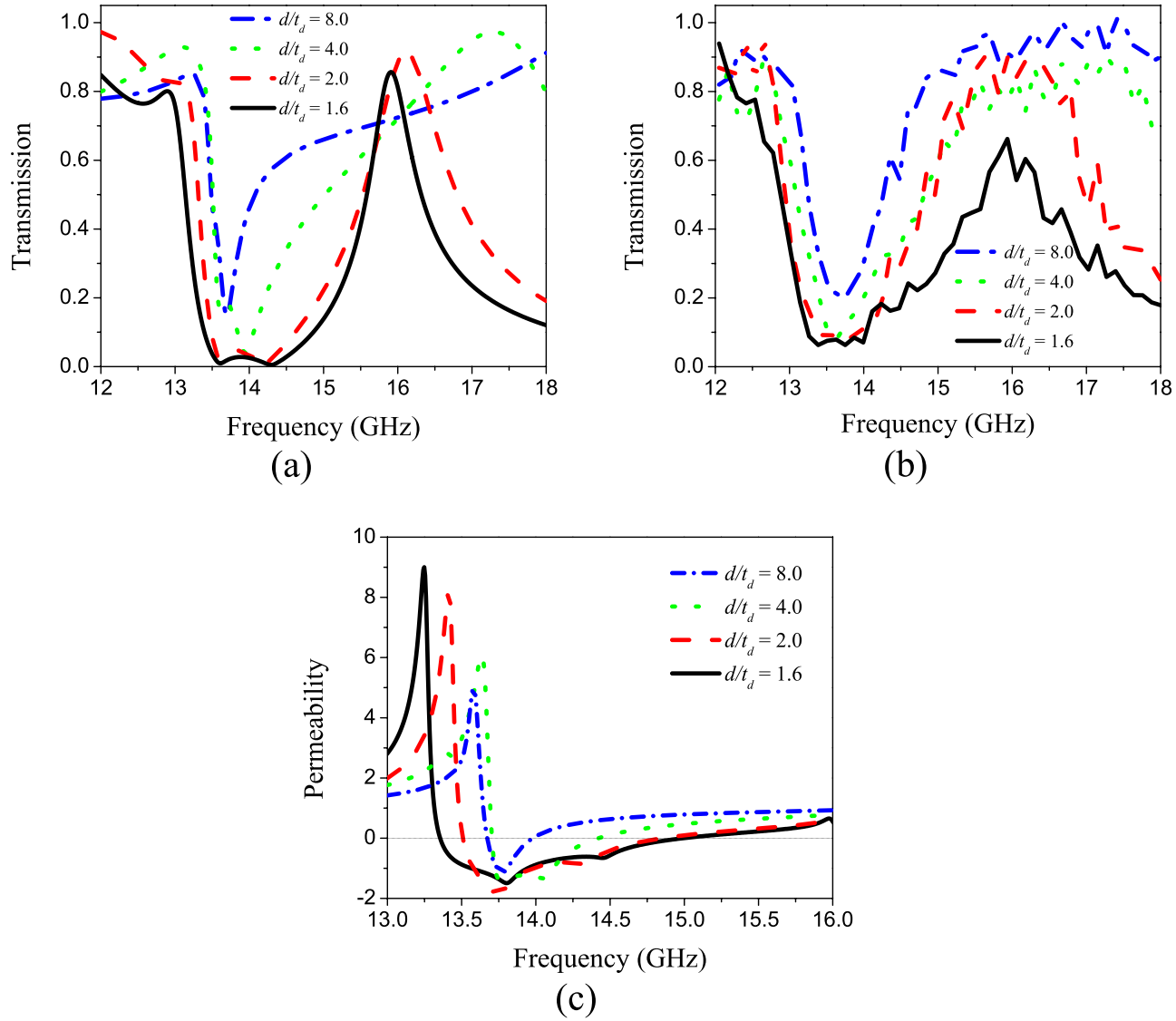

FIG. 4. (a) Simulated and (b) experimental transmissions according to d/t_d. (c) Dependence of calculated permeability on d/t_d. d is kept at 1.6 mm while t_d is varied. All other parameters are unchanged.

agreement with previous simulation work,[12] the results in Figs. 3(c) and 4(c) demonstrate that d/t_d is the decisive factor for governing the hybridization strength in CWP dimer systems.

So far, we know that the second-order hybridization scheme can be used to explain the hybridization of CWP dimers. One can now explore more complex interactions in multiple hybridized CWP systems. In Fig. 5, we present an effective medium analysis of a hybridized CWP trimer consisting of three identical CWP monomers. The distance between two consecutive monomers is 0.4 mm. To investigate the role of each CWP monomer in the system, each CWP monomer can be disabled by shortening two ends of the CWs. It is seen that for the unshorted CWP trimer the original resonance splits into three sub-resonances (transmission minima at 13.2, 13.5, and 14.4 GHz) and the resonant band is very broad. When the contribution of any of the three monomers is absent, the bandwidth is reduced. The magnitude of the reduction depends on the hybridization that occurs between the two remaining CWPs. In particular, the transmission in case of switching off the first CWP monomer totally coincides with the transmission in case of switching off the last one. The remaining systems behave like identical CWP dimers. This suggests that the electromagnetic behavior of the trimer can be considered as a (third-order) hybridization of a monomer and a dimer. The transmission is different when the middle CWP monomer is disable. In this case, the remaining system also acts like a weakly hybridized CWP dimer due to the longer distance d from the first to the last CWP monomer. It turns out that the original resonance is only slightly split (with transmission minima at 13.4 and 14.1 GHz) and the resonant band is obviously narrower than that of the two consecutive monomers.

The transmission behavior of the CWP trimer can be explained by the third-order hybridization scheme shown in Fig. 6. The original magnetic mode $|w_-\rangle$ of the monomer interacts with two individual modes of the dimer, $|w_{-+}\rangle$ and $|w_{--}\rangle$,

[This article is copyrighted as indicated in the article. Reuse of AIP content is subject to the terms at: http://scitation.aip.org/termsconditions. Downloaded to] IP: 84.194.89.79 On: Mon, 25 Aug 2014 18:07:57

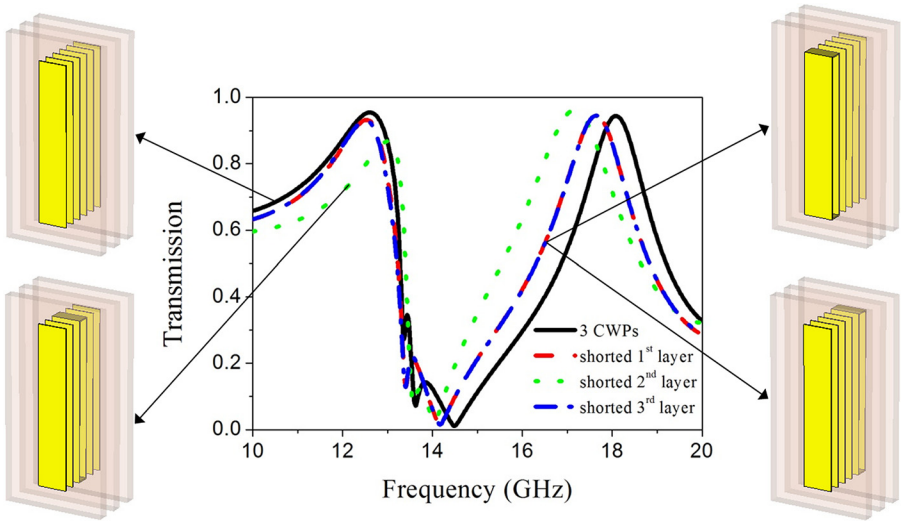

FIG. 5. Simulated transmission of a CWP trimer structure and of three CWP layers in which either the first, the second, or the third CWP layer is shorted.

stimulating four eigenmodes ($|w_{-++}\rangle$, $|w_{-+-}\rangle$, $|w_{--+}\rangle$, and $|w_{---}\rangle$). Since $|w_{-+-}\rangle$ and $|w_{--+}\rangle$ have the same energy, which is almost equal to that of $|w_{-}\rangle$, there finally are three different resonances in the transmission of the CWP trimer (as observed in Fig. 5). It should also be noted that the lower-frequency resonances are weaker due to the suppression of the positive permeability band of the higher-frequency resonances. By employing a N-mer CWP system, whose electromagnetic response can be explained as a hybridization of a monomer and a $(N-1)$-mer, the negative permeability band therefore can be further extended.

In addition to the potential applications in the microwave regime, broadband MMs at terahertz frequencies are attractive,[6–8,21] but at the same time challenging to construct. A general approach to obtain the optical counterpart of the microwave CWP dimer is to scale down all geometrical parameters of the microwave designs. The simulated transmission spectra and the simulated magnetic energy distributions of CWP monomer and dimer structures according to different scaling factors relative to the sizes defined in Sec. II are presented in Fig. 7. In these simulations, all the sizes mentioned in Sec. II are shrank down simultaneously by a factor of 0.15, 0.015, and 0.0015. For simplicity, no substrate has been considered in the simulations. The dielectric constant of the dielectric spacer is unchanged.

When the scaling factor is reduced from 0.15 to 0.0015, the hybridization still is obvious. For all scaling factors, the resonance bands of the CWP dimers are significantly broader than those of the CWP monomers. The induced magnetic energy concentrates mainly at the center of the CWPs, verifying the magnetic behavior of the resonance. Although the result in Fig. 7 shows a linear relation between the resonance frequency and the scaling factor, one should keep in mind that the linearity will break down for frequencies above 100 THz due to the free electron kinetic energy.[22,23] It is also forewarned by the transmission spectra of CWPs where the resonance becomes weaker and weaker when the resonance frequencies move toward the terahertz regime. Higher frequency resonances are more challenging not only because the dissipation for the increasing optical losses but also because the scaled-down

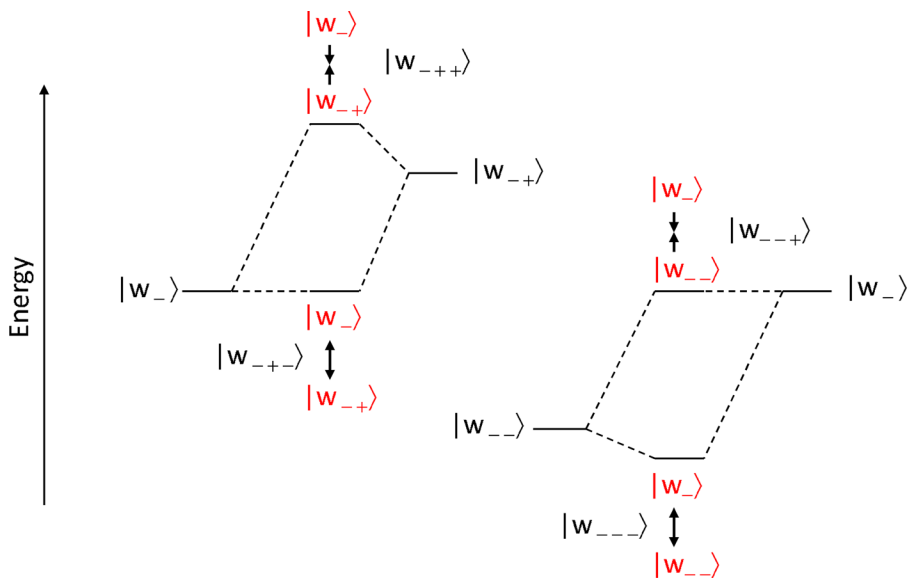

FIG. 6. Hybridization scheme of a CWP trimer.

[This article is copyrighted as indicated in the article. Reuse of AIP content is subject to the terms at: http://scitation.aip.org/termsconditions. Downloaded to] IP: 84.194.89.79 On: Mon, 25 Aug 2014 18:07:57

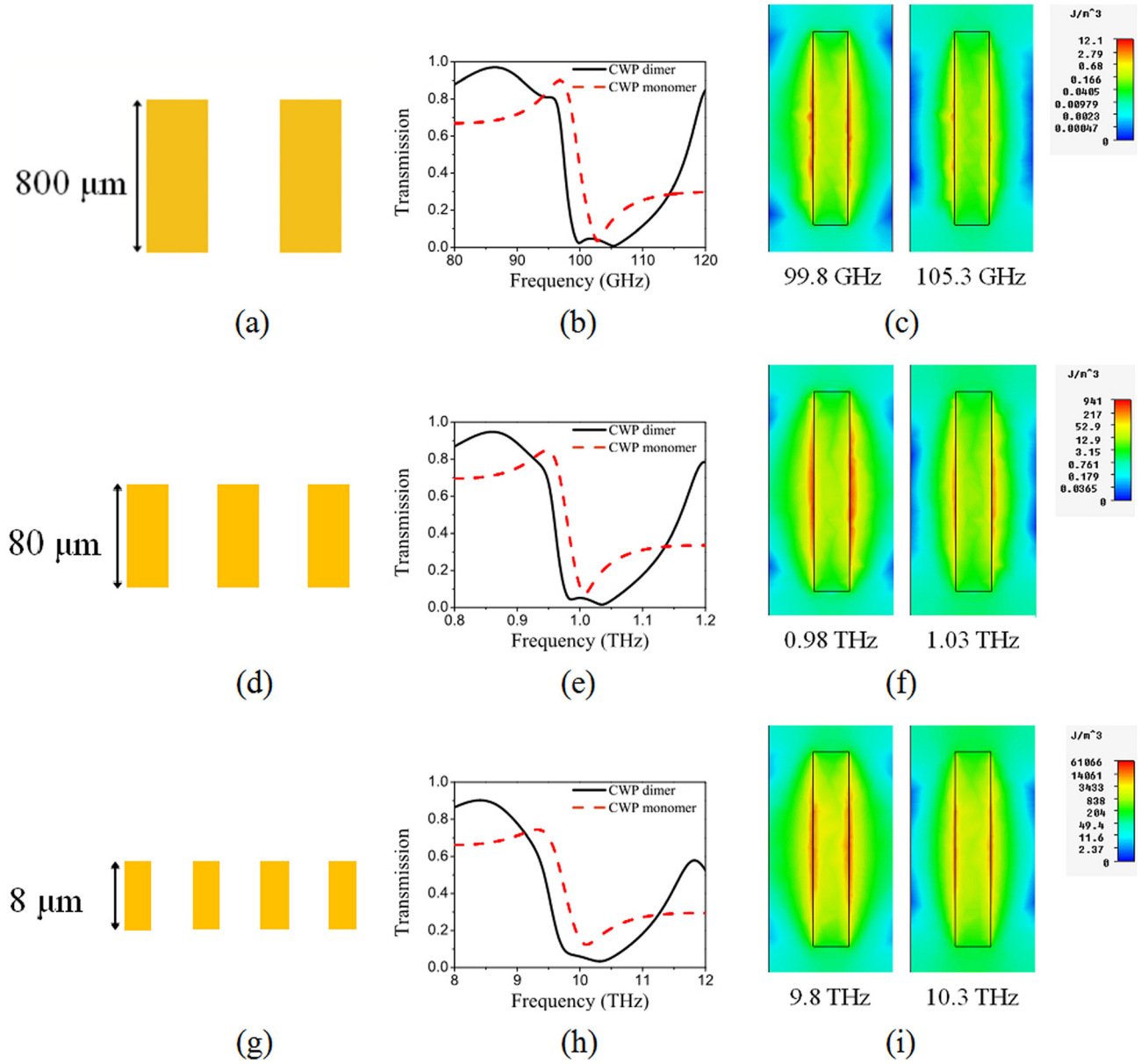

FIG. 7. Structure, simulated transmission spectrum, and simulated magnetic energy distribution of the CWP dimer corresponding to different scaling factors: (a)–(c) 0.15, (d)–(f) 0.015, and (g)–(i) 0.0015.

geometrical parameters might have to cross the state-of-the-art nanofabrication technologies.

IV. CONCLUSION

Broadband negative-permeability, based on second-order hybridized CWP dimers, is elaborated by systematic simulations and experiments in the microwave regime. It is demonstrated that the hybridization strongly depends on the interplay between the internal and external coupling of the dimers. It is found that the resonance split is activated when the strength of the internal coupling is comparable to that of the external coupling. An effective medium analysis is performed to generalize the hybridization scheme for more complex CWP arrangements. Finally, a full-scale simulation of hybridized CWP dimers indicates an independence of the broadband negative-permeability behavior on the scaling factor up to 10 THz.

ACKNOWLEDGMENTS

This research was funded by Vietnam National Foundation for Science and Technology Development (NAFOSTED) under Grant No. "103.02-2013.54" and the Research Foundation Flanders (FWO) FWO.2011.35.

[1]D. R. Smith, W. J. Padilla, D. C. Vier, S. C. Nemat-Nasser, and S. Schultz, Phys. Rev. Lett. **84**, 4184 (2000).
[2]J. B. Pendry, Phys. Rev. Lett. **85**, 3966 (2000).
[3]J. B. Pendry, A. J. Holden, W. J. Stewart, and I. Youngs, Phys. Rev. Lett. **76**, 4773 (1996).
[4]J. Zhou, E. N. Economon, Th. Koschny, and C. M. Soukoulis, Opt. Lett. **31**, 3620 (2006).
[5]Y. Luo, H. X. Peng, F. X. Qin, M. Ipatov, V. Zhukova, A. Zhukov, and J. Gonzalez, Appl. Phys. Lett. **103**, 251902 (2013).
[6]D. H. Kwon, D. H. Werner, A. V. Kildishev, and V. M. Shalaev, Opt. Express **15**, 1647 (2007).
[7]Z. Wei, Y. Cao, J. Han, C. Wu, Y. Fan, and H. Li, Appl. Phys. Lett. **97**, 141901 (2010).

[This article is copyrighted as indicated in the article. Reuse of AIP content is subject to the terms at: http://scitation.aip.org/termsconditions. Downloaded to] IP: 84.194.89.79 On: Mon, 25 Aug 2014 18:07:57

[8]C. Hu, L. Liu, X. N. Chen, and X. G. Luo, Opt. Express **16**, 21544 (2008).
[9]F. Ding, Y. Cui, X. Ge, Y. Jin, and S. He, Appl. Phys. Lett. **100**, 103506 (2012).
[10]Y. Cui, K. H. Fung, J. Xu, H. Ma, Y. Jin, S. He, and N. X. Fang, Nano Lett. **12**, 1443 (2012).
[11]D. R. Smith, D. C. Vier, Th. Koschny, and C. M. Soukoulis, Phys. Rev. E **71**, 036617 (2005).
[12]N. T. Tung, D. T. Viet, B. S. Tung, N. V. Hieu, P. Lievens, and V. D. Lam, Appl. Phys. Express **5**, 112001 (2012).
[13]V. D. Lam, N. T. Tung, M. H. Cho, J. W. Park, J. Y. Rhee, and Y. P. Lee, J. Appl. Phys. **105**, 113102 (2009).
[14]N. T. Tung, V. D. Lam, J. W. Park, M. H. Cho, J. Y. Rhee, W. H. Jang, and Y. P. Lee, J. Appl. Phys. **106**, 053109 (2009).
[15]E. Prodan, C. Radloff, N. J. Halas, and P. A. Nordlander, Science **302**, 419 (2003).
[16]A. Christ, O. J. F. Martin, Y. Ekinci, N. A. Gippius, and S. G. Tikhodeev, Nano Lett. **8**, 2171 (2008).
[17]B. Kante, S. N. Burokur, A. Sellier, A. D. Lustrac, and J. M. Lourtioz, Phys. Rev. B **79**, 075121 (2009).
[18]V. T. T. Thuy, D. T. Viet, N. V. Hieu, Y. P. Lee, V. D. Lam, and N. T. Tung, Opt. Commun. **283**, 4303 (2010).
[19]X. Chen, T. M. Grzegorczyk, B. I. Wu, J. Pacheco, and J. A. Kong, Phys. Rev. E **70**, 016608 (2004).
[20]V. D. Lam, N. T. Tung, M. H. Cho, J. W. Park, W. H. Jang, and Y. P. Lee, J. Phys. D: Appl. Phys. **42**, 115404 (2009).
[21]J. Cong, B. Jun, and Y. Cui, Opt. Express **21**, 20363 (2013).
[22]R. S. Penciu, M. Kafesaki, Th. Koschny, E. N. Economou, and C. M. Soukoulis, Phys. Rev. B **81**, 235111 (2010).
[23]J. Zhou, Th. Koschny, M. Kafesaki, E. N. Economou, J. B. Pendry, and C. M. Soukoulis, Phys. Rev. Lett **95**, 223902 (2005).

[This article is copyrighted as indicated in the article. Reuse of AIP content is subject to the terms at: http://scitation.aip.org/termsconditions. Downloaded to] IP: 84.194.89.79 On: Mon, 25 Aug 2014 18:07:57